Cellular/Molecular

Purinergic and Vanilloid Receptor Activation Releases Glutamate from Separate Cranial Afferent Terminals in Nucleus Tractus Solitarius

Young-Ho Jin,[1] Timothy W. Bailey,[1] Bai-yan Li,[2] John H. Schild,[2] and Michael C. Andresen[1]

[1]Department of Physiology and Pharmacology, Oregon Health and Science University, Portland, Oregon 97239-3098, and [2]Biomedical Engineering Program, Indiana University–Purdue University, Indianapolis, Indiana 46202-5132

Vanilloid (VR1) and purinergic (P2X) receptors are found in cranial afferent neurons in nodose ganglia and their central terminations within the solitary tract nucleus (NTS), but little is known about their function. We mechanically dissociated dorsomedial NTS neurons to preserve attached native synapses and tested for VR1 and P2X function primarily in spindle-shaped neurons resembling intact second-order neurons. All neurons ($n = 95$) exhibited spontaneous glutamate (EPSCs) and GABA (IPSCs)-mediated synaptic currents. VR1 agonist capsaicin (CAP; 100 nM) reversibly increased EPSC frequency, effects blocked by capsazepine. ATP (100 μM) increased EPSC frequency, actions blocked by P2X antagonist pyridoxalphosphate-6-azophenyl-2′, 4′-disulfonic acid (PPADS; 20 μM). In all CAP-resistant neurons, P2X agonist $\alpha\beta$-methylene-ATP ($\alpha\beta$-m-ATP) increased EPSC frequency. Neither CAP nor $\alpha\beta$-m-ATP altered EPSC amplitudes, kinetics, or holding currents. Thus, activation of VR1 and P2X receptors selectively facilitated presynaptic glutamate release on different NTS neurons. PPADS and 2′,3′-O-(2,4,6-trinitrophenyl)-ATP blocked $\alpha\beta$-m-ATP responses, but P2X1-selective antagonist NF023 (8,8′-[carbonylbis (imino-3,1-phenylene carbonylimino)]bis-1,3,5-naphthalenetrisulfonic acid) did not. The pharmacological profile and transient kinetics of ATP responses are consistent with P2X3 homomeric receptors. TTX and Cd^{2+} did not eliminate agonist-evoked EPSC frequency increases, suggesting that voltage-gated sodium and calcium channels are not required. In nodose ganglia, CAP but not $\alpha\beta$-m-ATP evoked inward currents in slow conducting neurons and the converse pattern in myelinated, rapidly conducting neurons ($n = 14$). Together, results are consistent with segregation of glutamatergic terminals into either P2X sensitive or VR1 sensitive that correspondingly identify myelinated and unmyelinated afferent pathways at the NTS.

Key words: **vanilloid; purinergic; presynaptic; glutamate; visceral afferent; brain stem**

Introduction

Unique expression patterns of particular ion channels or receptors often distinguish functional phenotypes within the nervous system. In sensory neurons of the dorsal root ganglion (DRG), the vanilloid (VR1) receptor (also designated TRPV1; Clapham et al., 2001) is closely associated with nociceptive afferent neurons, and VR1 plays a key role in sensory transduction. VR1 receptors and nociception in DRG have been linked to purinergic (P2X) receptors (Ralevic and Burnstock, 1998; Tominaga et al., 1998; Guo et al., 1999; Burnstock, 2000; Caterina and Julius, 2001). Individual adult DRG neurons are commonly responsive to both P2X and VR1 agonists (Li et al., 1999; Oh et al., 2001; Petruska et al., 2002; Labrakakis et al., 2003). Neonatal capsaicin lesion of VR1 DRG neurons greatly reduces P2X3 immunoreactivity in lamina II of dorsal horn (Vulchanova et al., 1998). Activation of both receptors on dorsal root afferent terminals in superficial lamina of the spinal cord facilitates glutamate release supporting functional colocalization (North, 2003a). The association of VR1 and P2X3 to nociception has attracted interest for their potential in pain therapeutic strategies (Eglen et al., 1999; Wood, 2000; North, 2003b).

VR1 and P2X3 receptors appear not to be limited to a nociceptive distribution, because they also localize to visceral afferent neurons that send axons via cranial nerves to the brain stem (Helliwell et al., 1998; Tominaga et al., 1998; Mezey et al., 2000). Cranial afferents such as those in nodose ganglion transduce conditions within heart, blood vessels, lungs, and other visceral organs. These cranial visceral primary afferents form the solitary tract (ST) within the brain stem, and their terminations mark second-order neurons within ST nucleus (NTS) (Loewy, 1990). At the light microscopic level, the afferent terminal fields within NTS appear strongly immunoreactive for VR1 (Guo et al., 1999) and P2X (Guo et al., 1999; Yao et al., 2001). Electron micrographic studies show that P2X3 receptors in NTS are located on presynaptic processes containing glutamate vesicles (Llewellyn-Smith and Burnstock, 1998) and modulate glutamatergic synaptic transmission (Kato and Shigetomi, 2001). Purinergic receptors in caudal NTS are required for normal cardiovascular reflexes (Ergene et al., 1994; Scislo et al., 1998; Paton et al., 2002).

Received Dec. 15, 2003; revised April 5, 2004; accepted April 9, 2004.

This work was supported by National Institutes of Health Grants HL-41119 (M.C.A.), HL-56460 (M.C.A.), and HL-70433 (T.W.B.).

Correspondence should be addressed to Dr. Michael C. Andresen, Department of Physiology and Pharmacology, Oregon Health and Science University, Portland, OR 97239-3098. E-mail: andresen@OHSU.edu.

DOI:10.1523/JNEUROSCI.0753-04.2004

 0270-6474/04/244709-09$15.00/0

Although the VR1-selective agonist capsaicin (CAP) triggers glutamate release onto some (i.e., CAP-sensitive) but not other (i.e., CAP-resistant) second-order NTS neurons (Doyle et al., 2002), the relationship of P2X receptors to VR1 receptors is unknown.

Here, we mechanically isolated NTS neurons with intact native synaptic terminals to test VR1 and P2X modulation of spontaneous EPSCs and tested agonist-evoked currents in primary afferent nodose neurons with defined conduction velocities. Specifically, we focused on determining whether P2X receptors alter glutamate release onto CAP-sensitive and CAP-resistant NTS neurons. Surprisingly, we found that, unlike superficial lamina of the spinal cord, VR1 and P2X receptors appear to be segregated to different glutamatergic terminals that contact separate pools of NTS neurons. Interestingly, this differential CNS expression of VR1 and P2X appears to correspond, respectively, to separate C- and A-type afferent pathways. These receptor patterns indicate pathway distinctions at the very first synapse of these brain stem pathways and potentially critical autonomic targets for drugs directed at vanilloid and purinergic receptors.

Materials and Methods

NTS slices. Hindbrains of male Sprague Dawley rats (2–3 weeks of age; Charles River, Wilmington, MA) were prepared as described previously (Doyle and Andresen, 2001). All animal procedures were conducted with the approval of the University Animal Care and Use Committee in accordance with the United States Public Health Service (PHS) Policy on Humane Care and Use of Laboratory Animals (PHS Policy) and the National Institutes of Health *Guide for the Care and Use of Laboratory Animals*. The hindbrain was removed and placed in ice-cold artificial CSF (ACSF) composed of (mM): 125 NaCl, 3 KCl, 1.2 KH_2PO_4, 1.2 $MgSO_4$, 25 $NaHCO_3$, 10 dextrose, 2 $CaCl_2$, and bubbled with 95% O_2/5% CO_2. The medulla was trimmed to a 1 cm block (rostral-caudal) centered on the obex (Doyle et al., 2004). The plane of section was adjusted by removing a wedge of tissue from the ventral surface to align the ST with the cutting plane when mounted in a vibrating microtome (VT-1000S; Leica, Nussloch, Germany). Slices (150–170 μm thick) cut in cold (0–2°C) ACSF with a sapphire knife (Delaware Diamond Knives, Wilmington, DE) contained the ST in the same plane as the NTS. The slices were then incubated (1–3 hr at 31°C) in ACSF before mechanical dispersion.

Mechanical dissociation of NTS neurons. To isolate NTS neurons, brain stem slices were transferred to 35 mm Petri dishes (Falcon 1008; Becton Dickinson, Franklin Lakes, NJ) filled with standard external recording solution containing the following (in mM): 150 NaCl, 5 KCl, 1 $MgCl_2$, 2 $CaCl_2$, 10 HEPES, and 10 glucose. The pH was adjusted to 7.4 with Tris-base, and recordings were at room temperature. A glass pipette was pulled to a fine tip and fire-polished to 100–120 μM (outer diameter). The pipette was mounted in a custom-made vibration device held by a micromanipulator. Neurons were harvested from restricted portions of the medial sub nucleus of NTS underlying the area postrema. The dispersion pipette was directed to portions of NTS medial to the visible solitary tract using a stereomicroscope, and the oscillating tip was lowered to the surface. The pipette oscillated (30 Hz) horizontally with excursions of 100–300 μm. The oscillating pipette tip was slowly moved using the micromanipulator to circumscribe an area of the subnucleus generally from the most caudal end of the fourth ventricle rostrally up to 500 μm and medial from the solitary tract to within 50 μm of the edge of the fourth ventricle, a region densely innervated with aortic baroreceptor terminals (Doyle and Andresen, 2001). Neurons were dissociated from the top 100 μm of the dorsal surface of the slices. The remainder of the slice was removed, and the dispersed neurons were allowed to settle and adhere to the bottom of the dish within 20 min. This subregion contains second-order neurons receiving both CAP-sensitive and CAP-resistant afferents from the solitary tract (Doyle et al., 2002).

NTS recording. Individual neurons were visualized using phase-contrast microscope (TE2000S; Nikon, Tokyo, Japan) with a 60× objective and a 10× ocular lens. Recordings of NTS neurons were made with an Axopatch 2B and pClamp 8 software (Axon Instruments, Foster City, CA) using nystatin-perforated patch electrodes (Akaike and Harata, 1994). Recording electrodes were filled with a solution composed of (mM): 50 KCl, 100 K gluconate, and 10 HEPES (with pH adjusted to 7.2 with Tris-base). The final concentration of nystatin was 450 μg/ml. NTS neurons dispersed in this manner have intact presynaptic boutons as indicated by the presence of spontaneous synaptic events (see Fig. 1), IPSCs and EPSCs. Only cells with holding currents of <60 pA and peak-to-peak noise levels of <4 pA were selected for detailed studies to assure the highest quality recordings. Currents were sampled every 20 μsec and saved to a computer.

Ganglion recordings of nodose neurons. To perform electrophysiological studies in nodose neurons with defined axonal conduction velocities (CVs), ganglia were isolated together with lengthy sections of the vagus nerve. Ganglion preparation methods have been described in detail previously (Li and Schild, 2002) and are only briefly presented here. Adult male Sprague Dawley rats (>150 gm) were deeply anesthetized (methoxyflurane; Schering-Plough Research Institute, Union, NJ), and nodose ganglia were exposed. The nodose ganglia and ~2 cm of vagal nerve trunk were carefully dissected using a stereomicroscope (40×) and excised bilaterally. The connective tissue capsules were exposed, and the ganglia incubated for 40 min at 37°C in an Earl's Balanced Salt Solution (EBSS; Sigma, St. Louis, MO) containing type 2 collagenase (1.0 mg/ml; Sigma). This was immediately followed by 20 min incubation at 37°C in EBSS containing trypsin (0.5 mg/ml; Sigma). The tissue was then placed in chilled (4–8°C) recording solution for at least 1 hr before study. Experiments used the patch-clamp technique to make recordings in both current and voltage clamp.

Nodose electrophysiology. Patch pipettes (7052; Corning, Corning, NY) were pulled (P-87; Sutter Instruments, Novato, CA) and polished (MF-830; Narishige, Tokyo, Japan) to a resistance of 1–1.5 MΩ. All experiments were performed using conventional whole-cell patch recordings and an Axopatch 700A amplifier (Axon Instruments). After the formation of a giga-ohm seal, the pipette capacitance and the total electrode access resistance (typically >3 MΩ) were compensated. Initially, vagally evoked somatic action potentials were recorded in current clamp using bridge mode. Bipolar stimulation of the vagus was delivered with wire hook electrodes using a 200 μsec suprathreshold constant current pulse. Afferent fiber CV was calculated as a ratio of conduction distance (nerve trunk length between the cathode of the stimulating electrode and the center of the ganglion) and the time interval in the recording trace between the stimulus artifact and the onset of the somatic action potential. The amplifier was then switched to voltage-clamp mode, and the cells were held at −60 mV to approximate normal resting membrane potential. Recording of total transmembrane current was initiated 10 sec before drug challenge and continued for 120–240 sec. All current-clamp data were low-pass filtered to 10 KHz and digitized at 40 KHz. All agonist-evoked currents measured in voltage clamp were low-pass filtered to 25 Hz and digitized at 50 Hz. The experimental protocols, data collection, and preliminary analysis were performed using pCLAMP 9 and the Digidata 1322A acquisition hardware (Axon Instruments).

Nodose recording solutions. The extracellular solution was prepared as a stock and consisted of (in mM): 137 NaCl, 5.4 KCl, 1 $MgCl_2$, 2 $CaCl_2$, 10 glucose, and 10 HEPES. The pH was adjusted to 7.3 using a measured quantity of 1N NaOH. The pipette solution was prepared as a stock and contained (in mM): 4 NaCl, 50 KCl, 50 K_2SO_4, 5 $MgCl_2$, and 10 HEPES. Just before recording, 2 mM each of Na-ATP and Na-GTP was added to the pipette solution along with 4 mM bis(2-aminophenoxy)ethane-*N*,*N*,*N*′,*N*′-tetra-acetic acid tetrapotassium salt (BAPTA-K; Sigma) and 0.25 $CaCl_2$ for a final buffered $[Ca^{2+}]_i$ of 10 nM. The pH was adjusted to 7.2 using 1N KOH. During the experiments, the pipette solution was kept from light and was chilled (8–12°C). Osmolarities of all extracellular and pipette solutions were adjusted using D-mannitol to 310 and 290 mOsm, respectively. All nodose experiments were performed at room temperature (20–23°C).

Drugs. CAP (100 nM), capsazepine (CZ; 500 nM), bicuculline methiodide (100 μM), 2,3-dihydroxy-6-nitro-7-sulfonyl-benzo[*f*]quinoxaline (NBQX; 20 μM), ATP (100 μM), the broad spectrum P2X-selective receptor antagonist pyridoxalphosphate-6-azophenyl-2′, 4′-disulfonic acid (PPADS; 10 μM), P2X1 receptor-specific antagonist (NF 023; 1 μM),

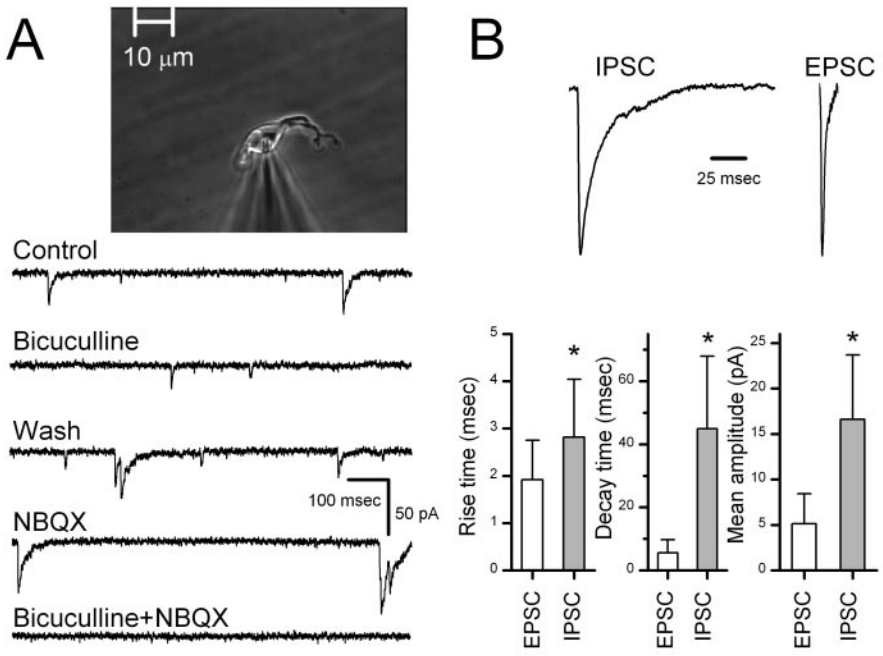

Figure 1. Synaptic responses recorded from a representative, acutely dispersed, medial NTS neuron. This neuron closely resembles second-order NTS neurons in its dimensions and spindle shape (inset). Spontaneous synaptic currents from this neuron were separated pharmacologically and kinetically into IPSCs and EPSCs. *A*, Pharmacological isolation of synaptic current subtypes within a single neuron. Control traces show large and small amplitude events. Bicuculline (100 μM) reversibly blocked large-amplitude, long-duration, synaptic currents (IPSCs) while preserving small-amplitude, brief synaptic currents (EPSCs). Wash returned to drug-free control solution. NBQX (20 μM) blocked EPSCs, but IPSCs remained. All synaptic currents were blocked by combined bicuculline and NBQX. *B*, Kinetic differences between bicuculline-sensitive IPSCs and NBQX-sensitive EPSCs from the same neuron as in *A*. Expanded traces illustrate that IPSCs (left) had prolonged time courses, whereas EPSCs (right) rapidly returned to baseline (amplitudes normalized to 100%). Average kinetic parameters for this neuron show that mean rise times (10–90%) and mean decay times were significantly shorter for EPSCs than IPSCs, and IPSC amplitudes (89 events) were larger than EPSCs (114 events). Bars represent mean ± SD; asterisks indicate significant differences ($p < 0.05$) by unpaired *t* test.

and AP-5 were obtained from Tocris Cookson (Ballwin, MO). CAP and CZ were dissolved in ethanol at 1 mM before diluting with external solution. The broad spectrum P2X-selective receptor antagonist 2′,3′-O-(2,4,6-trinitrophenyl) (TNP)-ATP (1 μM) and $\alpha\beta$-methylene ($\alpha\beta$-m)-ATP (10 μM) was obtained from Sigma-RBI (Natick, MA). TTX (3 μM) from Alomone Labs (Jerusalem, Israel) and Cd^{2+} (200 μM) from Sigma-RBI were added to block voltage-gated Na^+ and Ca^{2+} channels, respectively, in some experiments. For isolated NTS neurons, drugs were applied via a Y-tube system that provided complete solution changes surrounding isolated neurons within 20 msec (Murase et al., 1989). In contrast, in the nodose ganglion slice experiments, drugs were perfused (~1 ml/min) through a simple micropipette positioned ~200 μm from the recorded cell (Li and Schild, 2002).

Data analysis. Data were analyzed off-line using pClamp (Axon Instruments) and Mini Analysis (version 5.0; Synaptosoft, Decatur, GA). Plotting and additional regression curve fitting were performed using Origin 7.5 (OriginLab, Northampton, MA). Data are presented as SEM. Cumulative distributions of miniature synaptic current amplitudes and frequencies were compared using the Kolmogorov–Smirnov (K-S test) nonparametric analysis. Differences were considered statistically significant for p values < 0.05. Differences in mean amplitude and frequency were tested by paired or unpaired *t* tests as appropriate (Statview 4.5; SAS Institute, Cary, NC). For some protocols, two-way ANOVA or repeated measures ANOVA was performed.

Results

In dispersed medial NTS neurons ($n = 95$), spontaneous synaptic currents indicated the intermittent release of neurotransmitter from synaptic terminals retained on the isolated cell bodies (Fig. 1). Second-order NTS neurons observed in brain stem slices are characteristically spindle shaped with single processes emerging from either pole of the neuron (Doyle and Andresen, 2001). In the present study (Fig. 1, micrograph inset), we harvested cells from this same medial region and selected small, spindle-shaped, dispersed neurons (~6 by 9 μm). Two classes of synaptic events could be distinguished in dispersed NTS neurons. These synaptic events had distinct kinetics and pharmacological sensitivities. Within single neurons, the shortest spontaneous synaptic events had smaller mean amplitudes than events with longer durations (Fig. 1*B*). The small-amplitude class of synaptic events activated and decayed faster than the large-amplitude class (Fig. 1*B*). The selective antagonist NBQX blocked only the faster synaptic currents and identified these as glutamatergic EPSCs acting on non-NMDA receptors (Fig. 1*A*). The $GABA_A$-selective antagonist bicuculline reversibly blocked the long-lasting synaptic currents that were thus identified as GABAergic IPSCs (Fig. 1*A*). Application of NBQX and bicuculline together eliminated all spontaneous synaptic activity. On average, pharmacological separation of synaptic events showed that mean EPSC amplitudes ($n =$ 23 neurons) were smaller than IPSCs (7.43 ± 0.7 pA vs 27.8 ± 3.5 pA) and had shorter rise times (2.31 ± 0.11 vs 3.19 ± 0.22 msec) and faster decay times (9.36 ± 0.82 vs 48.12 ± 3.56 msec) than for IPSCs ($n = 18$ neurons). Zero Mg^{2+} conditions failed ($p > 0.05$) to alter EPSC amplitudes (107.2 ± 39% control), rise times (90.7 ± 38% control), or decay times (103.8 ± 55% control), and subsequent application of NBQX blocked all EPSCs. Our study will focus on such EPSCs isolated by the continuous presence of bicuculline.

Within medial NTS, ST-evoked EPSCs are either facilitated and then fully blocked by nanomolar concentrations of CAP (CAP sensitive) or are not altered (CAP resistant) (Doyle et al., 2002). In dispersed NTS neurons, CAP (100 nM) increased the frequency of spontaneous EPSCs in 16 of 26 cells tested (Fig. 2). CAP abruptly increased the frequency of EPSCs, and this increase peaked within the first 10–30 sec before declining in the continued presence of CAP. Return to control perfusate promptly returned the spontaneous EPSC rate to control levels (Fig. 2). Typically, EPSC frequency increased threefold to fivefold in CAP-sensitive neurons (Fig. 2). K-S testing of records from individual neurons showed consistent and significant ($p < 0.001$) increases in frequency but not in amplitudes. On average ($n =$ 14), CAP increased EPSC frequency to 569.8 ± 20.2% of control (paired *t* test; $p < 0.001$). CAP did not change EPSC mean amplitudes ($p = 0.45$; 95.8 ± 14.3% control), rise times ($p = 0.12$; 93.4 ± 5.2% control), or decay times ($p = 0.33$; 92.1 ± 11.5% control) in these CAP-sensitive neurons. The VR1 receptor-specific antagonist CZ (500 nM) reversibly blocked the CAP effect ($n = 2$) (Fig. 2). Holding currents were unaltered by CAP ($n =$ 14; $p = 0.14$; −29.8 ± 3.8 pA vs −30.4 ± 3.6 pA). In CAP-resistant neurons ($n = 10$), the spontaneous EPSC frequency was

unaffected by CAP ($p = 0.95$; 99.1 ± 24.2% control). Together, the results suggest that CAP selectively evokes a release of glutamate from presynaptic terminals on a subset of NTS neurons.

ATP (100 μM) increased the spontaneous frequency of EPSCs sixfold on average in responsive NTS neurons (7 of 15 tested) from 0.45 ± 0.17 to 3.55 ± 1.82 Hz without altering amplitudes ($p > 0.44$) or holding currents ($p > 0.36$). The broad-spectrum P2X antagonist PPADS (20 μM) blocked the actions of ATP on EPSC frequency in ATP responsive neurons ($p > 0.05$; $n = 4$) (Fig. 3). Likewise, the nonhydrolysable P2X receptor agonist αβ-m-ATP (10 μM) rapidly increased the spontaneous frequency of EPSCs in responsive neurons (13 of 24 tested) (Fig. 4*Aa*). K-S testing of records from individual neurons showed consistent and significant ($p < 0.001$) increases in EPSC frequency during ATP or αβ-m-ATP ($p < 0.0001$; $n = 10$; 557 ± 10.4% of control) but not in amplitudes ($p > 0.05$). Such response patterns were qualitatively similar to CAP responses in CAP-sensitive neurons. After returning to control perfusate, the EPSC frequency quickly fell to baseline (Fig. 4*Aa*). αβ-m-ATP failed to alter amplitudes ($p = 0.16$; 88.6 ± 12.9% control), rise times ($p = 0.69$; 99.6 ± 9.0% control), decay times ($p = 0.29$; 94.3 ± 9.4% control), or holding currents (−26.5 ± 3.8 pA vs −26.7 ± 3.4 pA; $p > 0.40$; $n = 11$). The kinetic response profile to agonist application provides an important clue as to the underlying subunit composition in purinergic receptors (Dunn et al., 2001), and the EPSC rate typically fell exponentially during αβ-m-ATP application with a decay constant of ~10 sec (Fig. 4*Ab*). PPADS (10 μM) blocked the αβ-m-ATP modulation of EPSCs in responsive neurons ($n = 3$) (Fig. 4*Aa*). The antagonist TNP-ATP (1 μM) blocked increases in EPSC frequency in a separate set of αβ-m-ATP responsive neurons ($n = 3$; control, 0.37 ± 0.09 Hz; αβ-m-ATP, 2.51 ± 0.88 Hz; αβ-m-ATP plus TNP-ATP, 0.34 ± 0.06 Hz). In an additional three αβ-m-ATP-responsive neurons, the P2X1-selective antagonist NF023 (1 μM) failed to alter the αβ-m-ATP-evoked increase in EPSC frequency (paired *t* test; $p = 0.36$).

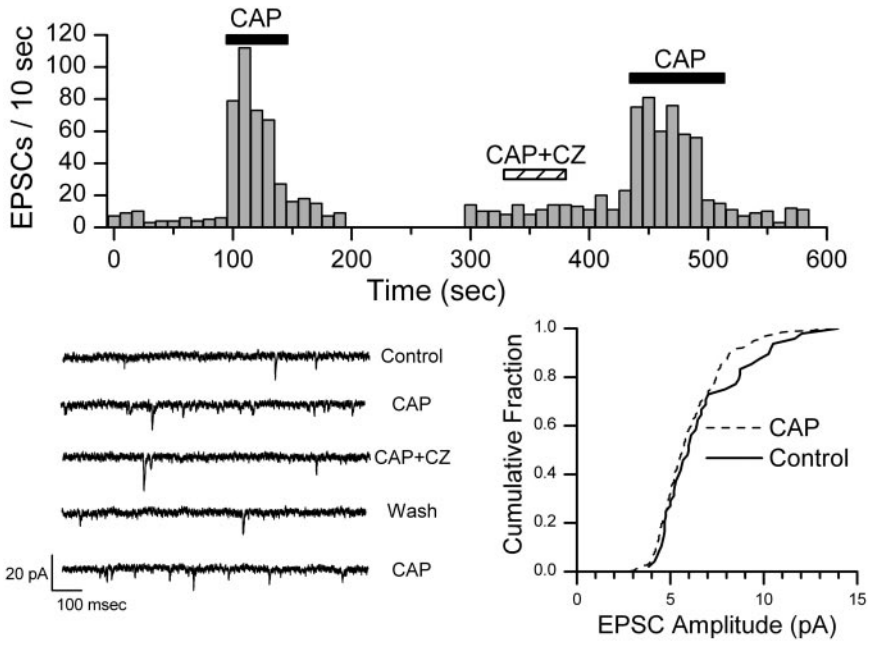

Figure 2. CAP increased the frequency of spontaneous EPSCs in this representative CAP-sensitive NTS neuron. Counts of EPSC events were collected over time bins of 10 sec. CAP (100 nM) rapidly and reversibly increased the rate of EPSCs, and this CAP effect was reversibly blocked by VR1 antagonist CZ (500 nM). Wash of CZ rapidly restored sensitivity to CAP. The histogram is an unbroken record of this single neuron. The bottom left panel shows examples of original, expanded current traces from this experiment in each condition. The bottom right panel shows that the distribution of amplitudes was unaltered by CAP (K-S test; $p > 0.05$). Bicuculline was present in all experiments.

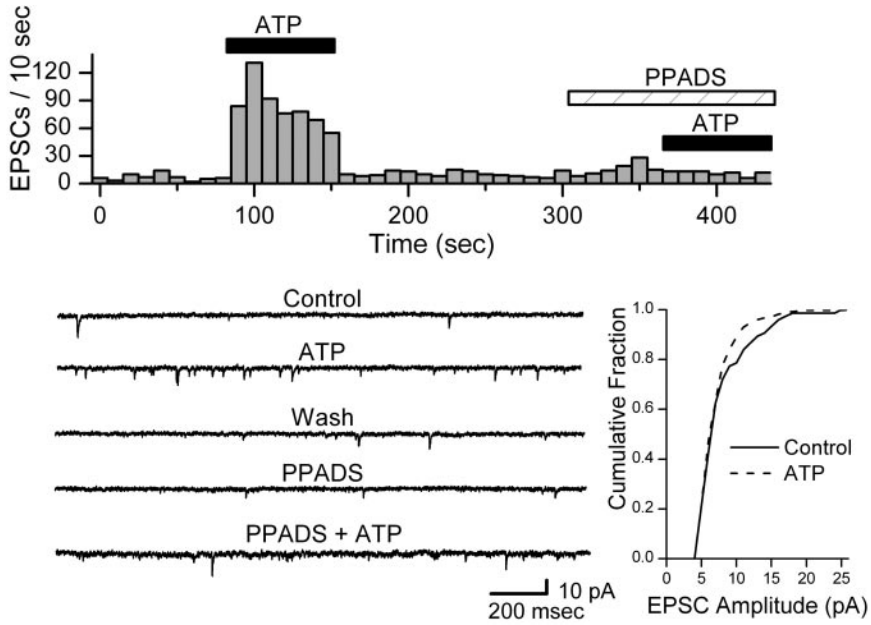

Figure 3. ATP increased the frequency of spontaneous EPSCs in ATP-sensitive NTS neurons. A representative protocol is displayed in the top panel. Counts of EPSC events were collected over time bins of 10 sec. ATP (100 μM) rapidly and reversibly increased the rate of EPSCs, and this effect was reversibly blocked by P2X antagonist PPADS (20 μM). ATP increased mean EPSC frequency (distribution not shown) from 0.61 Hz in control to 9.42 Hz (K-S test; $p = 0.0001$). The bottom left panel shows examples of original, expanded current traces from this experiment in each condition. The bottom right panel shows that ATP did not alter the cumulative distribution of amplitudes in this neuron (K-S test; $p > 0.05$). All data came from same neuron, and bicuculline was present in all conditions.

Activation of VR1 or P2X receptors triggered specific increases in the release rate of glutamatergic terminals of medial NTS neurons. In additional experiments, we tested whether EPSCs within single neurons were responsive to both VR1 and P2X agonists. All CAP-resistant neurons ($n = 8$) responded to αβ-m-ATP with an evoked increase in EPSC frequency (Fig. 5). Conversely, CAP-sensitive neurons ($n = 8$) were αβ-m-ATP resistant (Fig. 5). In three neurons, both CAP and αβ-m-ATP evoked increases in EPSC frequency. In none of these cases was EPSC amplitude (85.2 ± 40.8% control), rise times (110.5 ± 6.5% control), decay times (110.0 ± 16.4% control), or

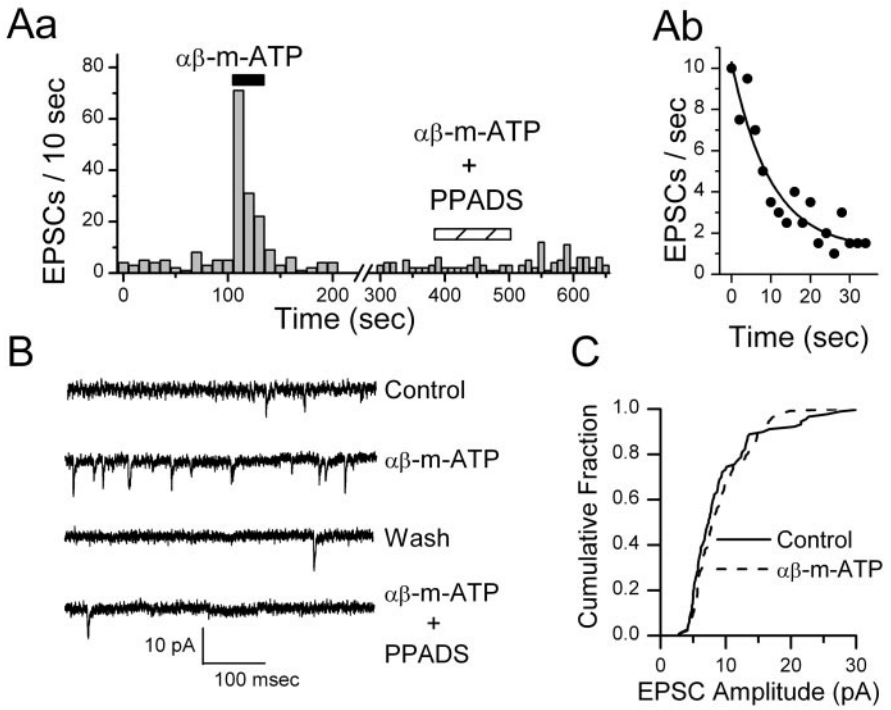

Figure 4. The nonmetabolized P2X agonist $\alpha\beta$-m-ATP (10 μM) quickly (*Aa*) and reversibly increased the rate of EPSCs in this ATP-sensitive NTS neuron, with the rate recovering quickly after agonist removal. Time bins were 10 sec. Analysis of the time course of the decrease in EPSC rate (points are EPSC events per 2 sec bin) during $\alpha\beta$-m-ATP (*Ab*) was best fit by a single exponential function depicted by the solid curve (Origin software). $y = A1^{-x/t1} + y0$; $\text{Chi}^2 = 0.99$; $R^2 = 0.89$; $y0 = 1.2 \pm 0.7$; $A1 = 9.1 \pm 0.8$; $t1 = 9.9 \pm 2.5$ sec. The P2X receptor antagonist PPADS (10 μM) reversibly blocked this effect (*Aa*). EPSC frequency increased from 0.5 to 2.4 Hz during $\alpha\beta$-m-ATP (K-S test; $p = 0.0003$). *B* displays examples of original, expanded current traces showing EPSCs in each condition for this purinergically sensitive neuron. *C* plots the distribution of EPSC amplitudes, and this was not altered by $\alpha\beta$-m-ATP ($p > 0.05$). Bicuculline was present in all experiments.

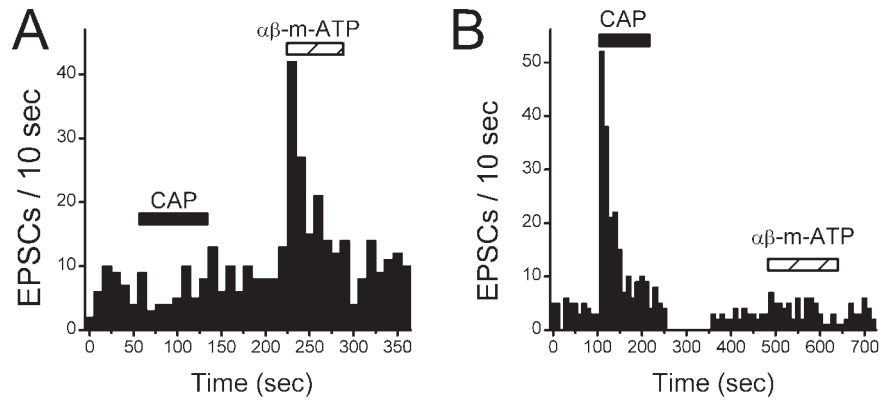

Figure 5. VR1 are located on presynaptic terminals of different NTS neurons than neurons with P2X receptors. Tests of CAP (100 nM) and $\alpha\beta$-m-ATP (10 μM) were made on single neurons to test whether both receptors could modulate glutamate release. The bin size was 10 sec for both histograms. Bicuculline was present in all experiments. *A*, In a CAP-resistant NTS neuron, CAP failed to alter the rate of spontaneous EPSCs, but $\alpha\beta$-m-ATP increased the rate of glutamate release. No amplitude changes were found. *B*, Conversely in a CAP-sensitive NTS neuron, CAP triggered increased EPSCs, but $\alpha\beta$-m-ATP (10 μM) was without effect. No amplitude changes were found.

holding currents (-13.5 ± 6.4 vs -14.2 ± 5.8 pA) significantly altered ($n = 3$; $p > 0.05$). The results suggest that glutamatergic afferents bearing VR1 receptors are generally distributed to a separate pool of NTS neurons than are glutamatergic terminals bearing P2X receptors.

Because we selected cells for study that morphologically resembled second-order NTS neurons in slices, we also tested the agonist responsiveness of neurons that did not fit this anatomical profile. EPSCs were recorded from three large neurons (mean dimensions, 8.33 ± 1.02 by 14.67 ± 0.82 μm) of irregular shape and relatively complicated proximal processes (three or more processes) compared with a pool of eight CAP-sensitive, spindle-shaped neurons (mean dimensions, 6.4 ± 0.5 by 8.8 ± 0.6 μm). Neither agonist altered EPSC amplitude ($96.1 \pm 37.3\%$ control), rise times ($98.5 \pm 10.7\%$ control), decay times ($80.6 \pm 18.2\%$ control), or holding currents (-22 ± 3.5 vs -21.7 ± 3.8 pA; $n = 3$; $p > 0.05$) for the spontaneous EPSCs recorded from these irregularly shaped neurons. In one of eight neurons tested, ATP (100 μM) reversibly induced an inward current of 55 pA without changing EPSC frequency ($104.1 \pm 10.7\%$ control; $p > 0.05$; $n = 8$).

VR1 and P2X receptors are coupled to poorly selective cation channels with relatively large Ca^{2+} permeabilities (Szallasi and Blumberg, 1999; Burnstock, 2000; Cunha and Ribeiro, 2000; Caterina and Julius, 2001; Khakh, 2001; Egan and Khakh, 2004; Shigetomi and Kato, 2004). Agonist activation of either receptor will depolarize presynaptic terminals, and this will activate voltage-dependent Na^+ and Ca^{2+} channels in the terminals. To assess the contribution of presynaptic voltage-dependent channels, we first tested agonist challenges to evoke glutamate release with and without TTX present to block presynaptic action potentials. TTX failed to alter the basal rate of spontaneous EPSCs (Fig. 6*a*) (0.50 ± 0.06 to 0.37 ± 0.10 Hz; $p = 0.22$; $n = 15$). In CAP-sensitive neurons in the presence of TTX, CAP initiated a sharp but brief burst of miniature EPSCs that was closely synchronized to the first 10 sec bin after CAP onset (Fig. 6*a*). In the absence of TTX (Fig. 6*a*), the increase in the EPSC rate was larger and more sustained (2.90 ± 1.15 vs 1.03 ± 0.23 Hz, CAP alone and CAP plus TTX, respectively; $n = 5$; $p = 0.04$). Similarly, in CAP-resistant neurons (Fig. 6*b*), $\alpha\beta$-m-ATP evoked peak EPSC responses in TTX that remained significant but were reduced (2.08 ± 0.62 vs 0.77 ± 0.12 Hz, control vs TTX, respectively; $n = 3$). Finally, we tested whether calcium entry after blockade of voltage-dependent calcium channels with 200 μM Cd^{2+} could modulate EPSC rates. In separate experiments, we compared agonist-triggered rates of release of glutamate in the presence of either TTX alone or with both TTX and Cd^{2+} (Fig. 6*a*,*b*). For CAP-sensitive neurons ($n = 5$), CAP triggered similar peak EPSC rate increases in TTX and in TTX plus Cd^{2+} (1.18 ± 0.23 vs 1.27 ± 0.43 Hz, respectively; $p > 0.05$). For ATP-sensitive neurons ($n = 4$), $\alpha\beta$-m-ATP triggered similar peak EPSC rate increases in TTX and in TTX plus Cd^{2+} (1.83 ± 0.44 vs 1.54 ± 0.33 Hz, respectively; $p > 0.05$). Thus,

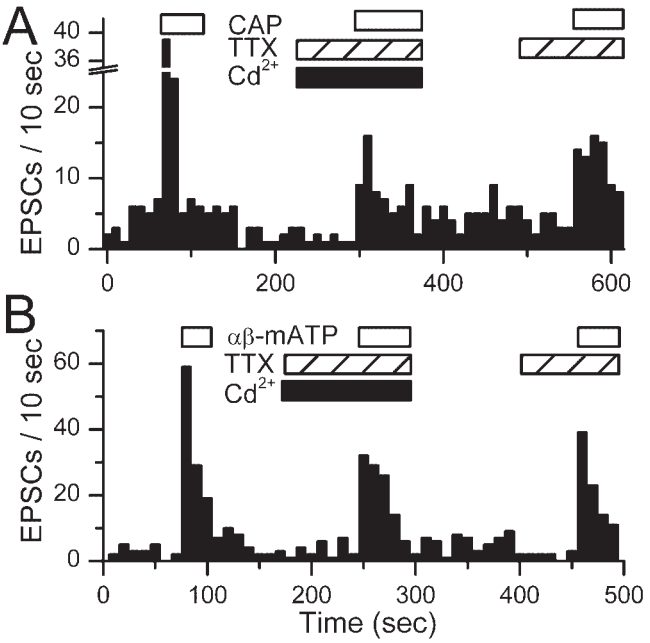

Figure 6. Voltage-dependent Na^+ and Ca^{2+} contribute to afferent glutamate release in VR1 and P2X responses. The bin size is 10 sec in histograms for each neuron. Bicuculline was present in all experiments. *A*, In a representative CAP-sensitive NTS neuron, application of CAP (100 nM) evoked a large transient increase in EPSCs (note broken y-axis). In the presence of both TTX (3 μM) and Cd^{2+} (200 μM), the CAP response was greatly reduced but not eliminated. Repeated CAP challenge in this same neuron with only TTX present evoked a similar peak response (amplitude of first 10 sec bin). *B*, In a representative CAP-resistant NTS neuron, $\alpha\beta$-m-ATP (10 μM) markedly increased the rate of spontaneous EPSCs. Such responses were greatly reduced but not eliminated by addition of TTX plus Cd^{2+} or TTX alone.

although TTX attenuated release from control, agonist could trigger similar release even when voltage-activated Ca^{2+} was blocked by Cd^{2+}. Together, these findings suggest that activation of either VR1 or P2X receptors conveyed sufficient Ca^{2+} influx to increase glutamate release at the two different types of NTS neurons.

Because the afferent glutamatergic terminals containing VR1 likely arise from slow conducting nodose sensory neurons, we tested whether nodose neurons expressed functional VR1 and P2X receptors and their relationship to axon type. For this, we recorded from nodose in a ganglion preparation in which we could activate the intact peripheral vagal nerve trunk (Fig. 7). Shocks to the vagus revealed two response types that corresponded to neurons with afferent axons classified as A- and C-types. A-type neurons exhibited characteristically short-duration action potentials, brief afterhyperpolarizations, and an average CV of 12.48 ± 1.30 m/sec ($n = 4$) (Fig. 7*A*). $\alpha\beta$-m-ATP (10 μM) evoked inward currents in all A-type nodose neurons, and these currents increased throughout the 150 sec of drug application. The $\alpha\beta$-m-ATP current at 150 sec averaged 860 ± 128 pA. None of these fast-conducting, myelinated afferent nodose neurons responded to 100 nM CAP. In contrast, all C-type neurons exhibited characteristically broad action potentials with long afterhyperpolarizations and slow CVs averaging 0.66 ± 0.13 m/sec ($n = 10$) (Fig. 7*B*). In all C-type neurons, CAP (100 nM) evoked an inward current that increased throughout the 150 sec of drug application reaching an average current of 1729 ± 907 pA. All C-type nodose neurons were unresponsive to $\alpha\beta$-m-ATP. No neurons were observed that were unresponsive to both agonists. Thus, adult nodose neurons appear to be either CAP sensitive and $\alpha\beta$-m-ATP resistant or CAP resistant and $\alpha\beta$-m-ATP sensitive, and these two pharmacological profiles correspond to neurons with C-type or A-type afferent axons, respectively.

Discussion

VR1 and P2X receptors facilitate glutamate release onto different NTS neurons

Our studies identify selective distribution patterns of presynaptic terminals containing either VR1 or P2X receptors within the medial NTS. Our nodose recordings provide direct evidence that this differential distribution of VR1 and P2X receptors is associated with unmyelinated and myelinated peripheral afferent pathways, respectively. Both of these receptor types are coupled to the release of glutamate. Interestingly, these VR1 and P2X receptors were rarely found on the same NTS neurons. Central processes from nodose neurons terminate in NTS (Andresen and Kunze, 1994). Here, we found that these afferent nodose neurons responded to either VR1 or P2X agonists but not both. Because the VR1-sensitive nodose neurons had uniformly very slow conduction velocities in the C-fiber range, we conclude that CAP-sensitive terminals in NTS correspond to presynaptic boutons of unmyelinated sensory afferents. Conversely, P2X-sensitive nodose neurons conducted in the A-fiber range and, therefore, P2X receptors mark the presynaptic NTS terminals of myelinated sensory afferents. Together, our findings suggest a fundamental segregation of VR1 from P2X receptors across afferent pathways to the medial NTS and little overlap or convergence at their central NTS neurons.

All neurons isolated from the dorsal medial portions of caudal NTS displayed spontaneous EPSCs, suggesting that glutamatergic boutons located on the soma and proximal dendrites are retained and functioning on the dispersed neurons. These EPSCs result from glutamate activation of non-NMDA receptors and thus are pharmacologically identical to synaptic transmission from ST afferents onto second-order NTS neurons (Doyle and Andresen, 2001). The presence of glutamatergic boutons on soma isolated from NTS is consistent with dye tracer studies showing that central terminations of cranial visceral afferents are concentrated nearest the cell bodies of second-order NTS neurons (Mendelowitz et al., 1992; Doyle and Andresen, 2001). The CAP-evoked EPSC responses that we recorded in isolated NTS neurons were identical to those observed in CAP-sensitive second-order NTS neurons in brain stem slices (Doyle et al., 2002). CAP actions at isolated neurons were blocked by VR1 antagonist CZ and increased the frequency of EPSCs without altering kinetics or amplitudes. Thus, the dispersed neurons morphologically and synaptically closely resemble second-order NTS neurons recorded in slices of this same region (Doyle and Andresen, 2001). CAP modulation of afferent glutamate release identifies two distinctive sets of second-order NTS neurons, CAP sensitive and CAP resistant (Bailey et al., 2002).

Given the association of VR1 and ATP with nociceptive afferent processing (Szallasi and Blumberg, 1999), we were surprised that ATP and its nonmetabolized analog $\alpha\beta$-m-ATP evoked EPSCs in every CAP-resistant NTS neuron. ATP and $\alpha\beta$-m-ATP rapidly and reversibly evoked glutamate release. The purinergic response characteristics were qualitatively very similar to those for vanilloid receptor activation in CAP-sensitive neurons. P2X activation increased EPSC frequency without altering amplitudes or kinetics in a similar manner to neurons recorded in NTS slices (Kato and Shigetomi, 2001). The lack of amplitude changes in our isolated NTS neurons suggests that ATP breakdown to adenosine does not contribute in the manner observed in slices (Kato

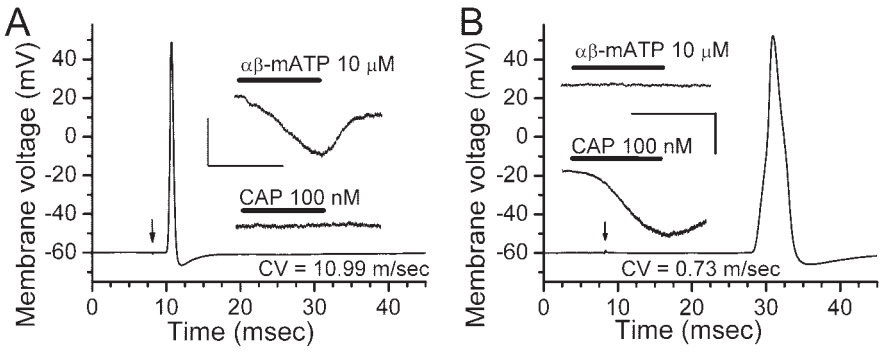

Figure 7. *A*, *B*, Vanilloid and purinergic sensitivity of nodose sensory neurons with myelinated (*A*) or unmyelinated (*B*) CVs. Vagal trunk stimulation (arrow) evoked a single somatic action potential in neurons recorded in current clamp and CV calculated. In the same neurons, current responses (insets) to both CAP (100 nM) and $\alpha\beta$-m-ATP (10 μM) were measured in voltage clamp at −60 mV. Bars indicate periods of drug perfusion. Horizontal and vertical scale bars for inset traces are 125 sec and 0.5 nA, respectively. *A*, Representative myelinated nodose neuron in which vagal stimulation evoked a characteristically narrow action potential with an afferent fiber CV of 10.99 m/sec. Inset, Top, Voltage-clamp currents show that microperfusion of $\alpha\beta$-m-ATP produced a strong inward current from this same neuron. Inset, Bottom, In contrast, CAP evoked no current in the same neuron. *B*, Vagal stimulation evoked a characteristically broad action potential with an afferent fiber CV of 0.73 m/sec in a representative unmyelinated nodose neuron. In contrast to the myelinated neurons, CAP evoked large inward current (inset), and $\alpha\beta$-m-ATP evoked no current in this same neuron (top inset).

and Shigetomi, 2001). The presynaptic actions of ATP and its analogs were blocked by PPADS and TNP-ATP. CAP-sensitive NTS neurons were generally unaffected by ATP agonists. P2X receptors at NTS neurons appear to be localized to presynaptic glutamate terminals that are distinct from those with VR1 and, interestingly, the CAP-sensitive and P2X-senstive terminals appear to be located on different NTS neurons.

The segregated pattern for VR1 and P2X receptors within NTS suggests that unmyelinated and myelinated afferent fibers follow separate paths to second-order brain stem neurons. This pattern in NTS appears to differ from the more mixed case for primary afferent processing in the spinal cord. In the spinal cord, C- and A-fiber terminals often converge on the same dorsal horn neurons (Yang et al., 1999). One third or more dorsal root neurons, the source for those dorsal horn afferent terminals, respond to both CAP and ATP (Zhong et al., 2001), although proportions vary across reports (Oh et al., 2001; Petruska et al., 2002; Labrakakis et al., 2003). Activation of P2X receptors in nearly all dorsal horn neurons transiently increases glutamate release (Nakatsuka et al., 2003), and most lamina II dorsal horn neurons are CAP sensitive (Nakatsuka et al., 2002). However, many P2X-sensitive afferent terminals in lamina V are CAP resistant (Tsuzuki et al., 2003). Thus, the patterns of VR1 and P2X receptor contributions to ionic currents in cranial visceral sensory afferent neurons as well as their synaptic transmission in NTS appear quantitatively very different from the corresponding response patterns for most spinal primary afferents and second-order neurons.

Presynaptic receptor mechanisms in NTS

Seven P2X receptor subunits have been identified, and functional homomeric and heteromeric receptors are distinguished pharmacologically and by their kinetics of activation and desensitization (Dunn et al., 2001; Khakh et al., 2001). The P2X3 subunit is of particular interest given its association with sensory neurons and their function (Deuchars, 2001). Evidence supports a localization for most of these individual subunits within NTS and nodose ganglion (Yao et al., 2000). In fact, electron microscopy has localized P2X3 subunits to presynaptic afferent terminals within NTS (Llewellyn-Smith and Burnstock, 1998). Less is known about local patterns of purinergic receptor expression within NTS regions or neuronal subtypes. Light microscopic studies have suggested immunohistochemical colocalization of P2X and VR1 within NTS (Vulchanova et al., 1997), although the intracellular epitope antibody (Ab) targets and detergent permeabilization may not distinguish membrane expression.

A difficult but important functional question to resolve with P2X receptors generally is the presence of homomeric and heteromeric purinergic receptors (Khakh et al., 2001). In cultured nodose neurons, P2X2/3 heteromultimeric channels likely exist along with homomeric P2X2 (Lewis et al., 1995; Virginio et al., 1998). For cultured neurons, the axotomy aspects of their isolation (Michael and Priestley, 1999) as well as the very young age of the source animals (Dunn et al., 2001) may influence substantially the receptor expression at the time of the assay. Our experiments focused on studies of NTS and nodose neurons acutely prepared from animals >14 d of age in an attempt to more closely match the conditions *in vivo*. $\alpha\beta$-m-ATP activates P2X1 and P2X3 subtypes, which rapidly desensitize (Lewis et al., 1995; Collo et al., 1996; Thomas et al., 1998), whereas the P2X2, P2X4, and P2X7 homomeric receptors desensitize slowly if at all (Dunn et al., 2001). P2X2/3 heteromers possess an $\alpha\beta$-m-ATP sensitivity similar to P2X3 homomers but with the slow desensitization kinetics of P2X2 (North and Surprenant, 2000; Dunn et al., 2001).

In our studies of glutamate release properties at NTS neurons, ATP and its analog $\alpha\beta$-m-ATP (maximally effective at 10 μM) triggered a pattern of EPSC activity that suggests P2X3 homomers. The evidence includes fast activation kinetics and a poorly sustained release during constant $\alpha\beta$-m-ATP stimulation. The desensitization time course (time constant of ~10 sec) and magnitude (nearly complete) resemble that of current responses evoked from P2X3 homomers. Recombinant P2X2 homomers have an EC_{50} for $\alpha\beta$-m-ATP >100 μM (Table 1 of Dunn et al., 2001). Likewise, the antagonist profile for blocking glutamate release onto these NTS neurons included complete blockade of release to maximally effective concentrations of $\alpha\beta$-m-ATP agonist at low concentrations of PPADS or TNP-ATP (a result that resembled that expected of P2X3 homomers, whereas P2X2 receptors generally require higher concentrations). The P2X1-selective antagonist NF023 failed to alter our purinergic responses. The very sluggish access of even directly and rapidly delivered drugs to the surface of the nodose ganglion (Li and Schild, 2002) prevented us from attempting analogous antagonist studies of these neurons, because the restricted drug access obscured assessment of receptor kinetics. The unresponsiveness of our slowly conducting nodose neurons to $\alpha\beta$-m-ATP differs from many reports suggesting broader expression in isolated nodose neurons, for example (Dunn et al., 2001). The reasons for this are not entirely clear, but the VR1/P2X segregation found in these relatively intact ganglion from adult rats clearly corresponded to the synaptic pharmacological profiles in NTS neurons. Caveats include potential differences in trafficking, assembly, and membrane incorporation of P2X subunits within cranial visceral afferents

and their three disparate domains (sensory endings, soma, and central terminals), subjects about which little is currently established. Differential expression at these three areas of the same neurons or across neurons of different sensory modality represents an interesting possibility. Nonetheless, for neurons within this medial region of NTS, the pharmacological sensitivity coupled with the rapid desensitization of our responses most closely resembles that expected of P2X3 homomers present in these afferent terminals (Khakh et al., 2001).

TTX failed to alter the rate of spontaneous EPSCs on our isolated NTS neurons, suggesting that, under these conditions, these events represent true miniature synaptic currents. However, agonist-triggered release was reduced by both TTX and Cd^{2+}, and thus under normal conditions, responses to activation of VR1 or P2X receptors appear to recruit voltage-dependent Na^{+} and Ca^{2+} channels in the process that facilitates release of glutamate. Because release persisted even in the presence of TTX and Cd^{2+}, we conclude that sufficient Ca^{2+} enters the presynaptic terminal via the open VR1 or P2X channels to result in facilitated release rates. Such results are consistent with the established high permeability to Ca^{2+} in both VR1 (Eglen et al., 1999) and P2X receptors (Virginio et al., 1998).

Differentiation of A- and C-fiber cranial afferent pathways

Our results provide evidence for fundamental differences in afferent pathways associated with primary visceral afferent fiber type at the first synapse within the brain stem. Two key receptors, P2X3 and VR1, appear to mark separate paths for myelinated A-fibers and unmyelinated C-fibers, respectively. Such segregation begins at the cell bodies of these primary visceral afferents within peripheral sensory ganglia and follows through to their central terminations with the brain stem at NTS. Interestingly, distinctions in the second-order NTS neurons themselves suggest that differential expression of potassium channels and differences in adaptive discharge properties are related to whether the neuron receives CAP-sensitive or CAP-resistant ST afferent input (Bailey et al., 2002). This pathway differentiation may offer insight to known differences in the functional performance of autonomic reflex pathways. For example, this dorsomedial region of NTS contains dense terminations of aortic baroreceptor afferents (Mendelowitz et al., 1992). Selective activation of either A- or C-type baroreceptors evokes reflex responses that differ markedly in their frequency-response relationships (Fan et al., 1999). The patterns of the afferent volley entering the CNS strongly effect the reflex outcome (Seagard et al., 1993; Fan and Andresen, 1998; Fan et al., 1999). Afferent bursts elicit greater reflex changes in blood pressure with A-type but not C-type afferents (Fan and Andresen, 1998). The mechanisms for these differences in reflex performance are unknown. However, microinjection of P2X antagonist in subpostremal NTS depressed the gain of the baroreflex, suggesting that sensitivity of the intact reflex depends on ongoing P2X receptor activity (Scislo et al., 1998). Thus, the differences of afferent-associated receptors offer potential mechanisms for pathway differentiation of performance beginning at the second-order neurons.

References

Akaike N, Harata N (1994) Nystatin perforated patch recording and its applications to analyses of intracellular mechanisms. Jpn J Physiol 44:433–473.

Andresen MC, Kunze DL (1994) Nucleus tractus solitarius: gateway to neural circulatory control. Annu Rev Physiol 56:93–116.

Bailey TW, Jin Y-H, Doyle MW, Andresen MC (2002) Vanilloid sensitive afferents activate neurons with prominent A-type potassium currents in nucleus tractus solitarius. J Neurosci 22:8230–8237.

Burnstock G (2000) P2X receptors in sensory neurones. Br J Anaesth 84:476–488.

Caterina MJ, Julius D (2001) The vanilloid receptor: a molecular gateway to the pain pathway. Annu Rev Neurosci 24:487–517.

Clapham DE, Runnels LW, Strubing C (2001) The TRP ion channel family. Nat Rev Neurosci 2:387–396.

Collo G, North RA, Kawashima E, Merlo-Pich E, Neidhart S, Surprenant A, Buell G (1996) Cloning OF P2X5 and P2X6 receptors and the distribution and properties of an extended family of ATP-gated ion channels. J Neurosci 16:2495–2507.

Cunha RA, Ribeiro JA (2000) ATP as a presynaptic modulator. Life Sci 68:119–137.

Deuchars J (2001) Knockout mice highlight the promise of purines. Trends Neurosci 24:5–6.

Doyle MW, Andresen MC (2001) Reliability of monosynaptic transmission in brain stem neurons *in vitro*. J Neurophysiol 85:2213–2223.

Doyle MW, Bailey TW, Jin Y-H, Andresen MC (2002) Vanilloid receptors presynaptically modulate visceral afferent synaptic transmission in nucleus tractus solitarius. J Neurosci 22:8222–8229.

Doyle MW, Bailey TW, Jin Y-H, Appleyard SM, Low MJ, Andresen MC (2004) Strategies for cellular identification in nucleus tractus solitarius slices. J Neurosci Methods, in press.

Dunn PM, Zhong Y, Burnstock G (2001) P2X receptors in peripheral neurons. Prog Neurobiol 65:107–134.

Egan TM, Khakh BS (2004) Contribution of calcium ions to P2X channel responses. J Neurosci 24:3413–3420.

Eglen RM, Hunter JC, Dray A (1999) Ions in the fire: recent ion-channel research and approaches to pain therapy. Trends Pharmacol Sci 20:337–342.

Ergene E, Dunbar JC, O'Leary DS, Barraco RA (1994) Activation of P_2-purinoceptors in the nucleus tractus solitarius mediate depressor responses. Neurosci Lett 174:188–192.

Fan W, Andresen MC (1998) Differential frequency-dependent reflex integration of myelinated and nonmyelinated rat aortic baroreceptors. Am J Physiol 275:H632–H640.

Fan W, Schild JH, Andresen MC (1999) Graded and dynamic reflex summation of myelinated and unmyelinated rat aortic baroreceptors. Am J Physiol 277:R748–R756.

Guo A, Vulchanova L, Wang J, Li X, Elde R (1999) Immunocytochemical localization of the vanilloid receptor 1 (VR1): relationship to neuropeptides, the $P2X_3$ purinoceptor and IB4 binding sites. Eur J Neurosci 11:946–958.

Helliwell RJA, McLatchie LM, Clarke M, Winter J, Bevan S, McIntyre P (1998) Capsaicin sensitivity is associated with the expression of the vanilloid (capsaicin) receptor (VR1) mRNA in adult rat sensory ganglia. Neurosci Lett 250:177–180.

Kato F, Shigetomi E (2001) Distinct modulation of evoked and spontaneous EPSCs by purinoceptors in the nucleus tractus solitarii of the rat. J Physiol (Lond) 530:469–486.

Khakh BS (2001) Molecular physiology of P2X receptors and ATP signalling at synapses. Nat Rev Neurosci 2:165–174.

Khakh BS, Burnstock G, Kennedy C, King BF, North RA, Seguela P, Voigt M, Humphrey PP (2001) International union of pharmacology. XXIV. Current status of the nomenclature and properties of P2X receptors and their subunits. Pharmacol Rev 53:107–118.

Labrakakis C, Tong CK, Weissman T, Torsney C, MacDermott AB (2003) Localization and function of ATP and GABAA receptors expressed by nociceptors and other postnatal sensory neurons in rat. J Physiol (Lond) 549:131–142.

Lewis C, Neidhart S, Holy C, North RA, Buell G, Surprenant A (1995) Co-expression of $P2X_2$ and $P2X_3$ receptor subunits can account for ATP-gated currents in sensory neurons. Nature 377:432–435.

Li BY, Schild JH (2002) Patch clamp electrophysiology in the nodose ganglia of the adult rat. J Neurosci Methods 115:157–167.

Li CY, Peoples RW, Lanthorn TH, Li ZW, Weight FF (1999) Distinct ATP-activated currents in different types of neurons dissociated from rat dorsal root ganglion. Neurosci Lett 263:57–60.

Llewellyn-Smith IJ, Burnstock G (1998) Ultrastructural localization of $P2X_3$ receptors in rat sensory neurons. NeuroReport 9:2545–2550.

Loewy AD (1990) Central autonomic pathways. In: Central regulation of autonomic functions (Loewy AD, Spyer KM, eds), pp 88–103. New York: Oxford.

Mendelowitz D, Yang M, Andresen MC, Kunze DL (1992) Localization and retention *in vitro* of fluorescently labeled aortic baroreceptor terminals on neurons from the nucleus tractus solitarius. Brain Res 581:339–343.

Mezey E, Toth ZE, Cortright DN, Arzubi MK, Krause JE, Elde R, Guo A, Blumberg PM, Szallasi A (2000) Distribution of mRNA for vanilloid receptor subtype 1 (VR1), and VR1-like immunoreactivity, in the central nervous system of the rat and human. Proc Natl Acad Sci USA 97:3655–3660.

Michael GJ, Priestley JV (1999) Differential expression of the mRNA for the vanilloid receptor subtype 1 in cells of the adult rat dorsal root and nodose ganglia and its downregulation by axotomy. J Neurosci 19:1844–1854.

Murase K, Ryu PD, Randic M (1989) Excitatory and inhibitory amino acids and peptide-induced responses in acutely isolated rat spinal dorsal horn neurons. Neurosci Lett 103:56–63.

Nakatsuka T, Furue H, Yoshimura M, Gu JG (2002) Activation of central terminal vanilloid receptor-1 receptors and alpha beta-methylene-ATP-sensitive P2X receptors reveals a converged synaptic activity onto the deep dorsal horn neurons of the spinal cord. J Neurosci 22:1228–1237.

Nakatsuka T, Tsuzuki K, Ling JX, Sonobe H, Gu JG (2003) Distinct roles of P2X receptors in modulating glutamate release at different primary sensory synapses in rat spinal cord. J Neurophysiol 89:3243–3252.

North RA (2003a) P2X3 receptors and peripheral pain mechanisms. J Physiol (Lond) 554:301–308.

North RA (2003b) The P2X3 subunit: a molecular target in pain therapeutics. Curr Opin Invest Drugs 4:833–840.

North RA, Surprenant A (2000) Pharmacology of cloned P2X receptors. Annu Rev Pharmacol Toxicol 40:563–580.

Oh SB, Tran PB, Gillard SE, Hurley RW, Hammond DL, Miller RJ (2001) Chemokines and glycoprotein120 produce pain hypersensitivity by directly exciting primary nociceptive neurons. J Neurosci 21:5027–5035.

Paton JFR, De Paula PM, Spyer KM, Machado BH, Boscan P (2002) Sensory afferent selective role of P2 receptors in the nucleus tractus solitarii for mediating the cardiac component of the peripheral chemoreceptor reflex in rats. J Physiol (Lond) 543 3:995–1005.

Petruska JC, Napaporn J, Johnson RD, Cooper BY (2002) Chemical responsiveness and histochemical phenotype of electrophysiologically classified cells of the adult rat dorsal root ganglion. Neuroscience 115:15–30.

Ralevic V, Burnstock G (1998) Receptors for purines and pyrimidines. Pharmacol Rev 50:413–492.

Scislo TJ, Ergene E, O'Leary DS (1998) Impaired arterial baroreflex regulation of heart rate after blockade of P_2-purinoceptors in the nucleus tractus solitarius. Brain Res Bull 47:63–67.

Seagard JL, Hopp FA, Drummond HA, Van Wynsberghe DM (1993) Selective contribution of two types of carotid sinus baroreceptors to the control of blood pressure. Circ Res 72:1011–1022.

Shigetomi E, Kato F (2004) Action potential-independent release of glutamate by Ca^{2+} entry through presynaptic P2X receptors elicits postsynaptic firing in the brainstem autonomic network. J Neurosci 24:3125–3135.

Szallasi A, Blumberg PM (1999) Vanilloid (capsaicin) receptors and mechanisms. Pharmacol Rev 51:159–212.

Thomas S, Virginio C, North RA, Surprenant A (1998) The antagonist trinitrophenyl-ATP reveals co-existence of distinct P2X receptor channels in rat nodose neurones. J Physiol (Lond) 509:411–417.

Tominaga M, Caterina MJ, Malmberg AB, Rosen TA, Gilbert H, Skinner K, Raumann BE, Basbaum AI, Julius D (1998) The cloned capsaicin receptor integrates multiple pain-producing stimuli. Neuron 21:531–543.

Tsuzuki K, Ase A, Seguela P, Nakatsuka T, Wang CY, She JX, Gu JG (2003) TNP-ATP-resistant P2X ionic current on the central terminals and somata of rat primary sensory neurons. J Neurophysiol 89:3235–3242.

Virginio C, North RA, Surprenant A (1998) Calcium permeability and block at homomeric and heteromeric $P2X_2$ and $P2X_3$ receptors, and P2X receptors in rat nodose neurones. J Physiol (Lond) 510:27–35.

Vulchanova L, Riedl MS, Shuster SJ, Buell G, Surprenant A, North RA, Elde R (1997) Immunohistochemical study of the P2X2 and P2X3 receptor subunits in rat and monkey sensory neurons and their central terminals. Neuropharmacology 36:1229–1242.

Vulchanova L, Riedl MS, Shuster SJ, Stone LS, Hargreaves KM, Buell G, Surprenant A, North RA, Elde R (1998) P2X3 is expressed by DRG neurons that terminate in inner lamina II. Eur J Neurosci 10:3470–3478.

Wood JN (2000) II. Genetic approaches to pain therapy. Am J Physiol Gastrointest Liver Physiol 278:G507–G512.

Yang K, Kumamoto E, Furue H, Li YQ, Yoshimura M (1999) Action of capsaicin on dorsal root-evoked synaptic transmission to substantia gelatinosa neurons in adult rat spinal cord slices. Brain Res 830:268–273.

Yao ST, Barden JA, Finkelstein DI, Bennett MR, Lawrence AJ (2000) Comparative study on the distribution patterns of P2X(1)-P2X(6) receptor immunoreactivity in the brainstem of the rat and the common marmoset (Callithrix jacchus): association with catecholamine cell groups. J Comp Neurol 427:485–507.

Yao ST, Barden JA, Lawrence AJ (2001) On the immunohistochemical distribution of ionotropic P2X receptors in the nucleus tractus solitarius of the rat. Neuroscience 108:673–685.

Zhong Y, Dunn PM, Bardini M, Ford AP, Cockayne DA, Burnstock G (2001) Changes in P2X receptor responses of sensory neurons from P2X3-deficient mice. Eur J Neurosci 14:1784–1792.